Am J Physiol Regul Integr Comp Physiol 295: R659–R668, 2008.
First published May 21, 2008; doi:10.1152/ajpregu.90357.2008.

Resistance to Ca^{2+}-induced opening of the permeability transition pore differs in mitochondria from glycolytic and oxidative muscles

Martin Picard,[2] Kristina Csukly,[1] Marie-Eve Robillard,[1] Richard Godin,[2] Alexis Ascah,[1] Céline Bourcier-Lucas,[1] and Yan Burelle[1]

[1]*Département de kinésiologie, Université de Montréal, Montreal, Quebec; and* [2]*Department of Kinesiology and Physical Education, McGill University, Montreal, Quebec, Canada*

Submitted 15 April 2008; accepted in final form 16 May 2008

Picard M, Csukly K, Robillard M-E, Godin R, Ascah A, Bourcier-Lucas C, Burelle Y. Resistance to Ca^{2+}-induced opening of the permeability transition pore differs in mitochondria from glycolytic and oxidative muscles. *Am J Physiol Regul Integr Comp Physiol* 295: R659–R668, 2008. First published May 21, 2008; doi:10.1152/ajpregu.90357.2008.—This study determined whether susceptibility to opening of the permeability transition pore (PTP) varies according to muscle phenotype represented by the slow oxidative soleus (Sol) and superficial white gastrocnemius (WG). Threshold for Ca^{2+}-induced mitochondrial Ca^{2+} release following PTP opening was determined with a novel approach using permeabilized ghost myofibers. Threshold values for PTP opening were approximately threefold higher in fibers from WG compared with those from Sol (124 ± 47 vs. 30.4 ± 6.8 pmol Ca^{2+}/mU citrate synthase). A similar phenomenon was also observed in isolated mitochondria (threshold: 121 ± 60 vs. 40 ± 10 nmol Ca^{2+}/mg protein in WG and Sol), indicating that this was linked to differences in mitochondrial factors between the two muscles. The resistance of WG fibers to PTP opening was not related to the expression of putative protein modulators (cyclophilin D, adenylate nucleotide translocator-1, and voltage-dependent anion channels) or to difference in respiratory properties and occurred despite the fact that production of reactive oxygen species, which promote pore opening, was higher than in the Sol. However, endogenous matrix Ca^{2+} measured in mitochondria isolated under resting baseline conditions was approximately twofold lower in the WG than in the Sol (56 ± 4 vs. 111 ± 11 nmol/mg protein), which significantly accounted for the resistance of WG. Together, these results reveal fiber type differences in the sensitivity to Ca^{2+}-induced PTP opening, which may constitute a physiological mechanism to adapt mitochondria to the differences in Ca^{2+} dynamics between fiber types.

skeletal muscle; fiber phenotype

THE MITOCHONDRIAL PERMEABILITY TRANSITION was initially described in isolated mitochondria as a sudden increase of the inner membrane permeability to solutes in the presence of a high Ca^{2+} concentration ($[Ca^{2+}]$) (24). Although initially thought to be due to unspecific membrane damage, this phenomenon is now widely accepted to actually be caused by the opening of the PTP, a nonspecific high-conductance proteinaceous channel of the inner membrane (14, 18, 22, 24, 25, 31, 51, 52). Prolonged opening of the PTP in the large-conductance mode leads to equilibration of ions and solutes of $<1{,}500$ Da across mitochondrial membranes, collapse of membrane potential ($\Delta\Psi$), mitochondrial swelling, and ATP hydrolysis by the F_0F_1ATPase. This sequence of events has drawn considerable attention to the PTP as an important player in apoptotic and necrotic cell death through at least three mechanisms: *1*) reduction in cellular ATP levels, *2*) increase in cytosolic Ca^{2+}, and *3*) release of several proapoptotic proteins normally sequestered in mitochondria, including cytochrome *c*, AIF, EndoG, Smac/Diablo, and Omi/HtrA2. Experimental evidence also has indicated that transient opening of the PTP (i.e., pore flickering) in a low-conductance mode that is permeable to ions but not to larger molecules may serve physiological regulatory purposes by fine-tuning $\Delta\Psi$ (33) and acting as a fast Ca^{2+} release channel that would regulate mitochondrial Ca^{2+} levels and participate in the amplification/propagation of Ca^{2+} signals arising from the endoplasmic (ER)-sarcoplasmic (SR) reticulum located near mitochondria (26, 30, 48).

Very few data are available on the regulation of the PTP in healthy skeletal muscle (20). One particularity of this tissue is that depending on the fiber type, large variations exist in the amount, size, and spatial configuration of mitochondria relative to the SR and myofibrils (40). Moreover, cellular Ca^{2+} dynamics are known to differ considerably across fiber types in both amplitude and frequency (6, 10, 11), which likely expose mitochondria to different levels of Ca^{2+}. Since Ca^{2+} loading of the matrix is the most important and obligatory trigger for PTP opening (51), it is possible that mitochondria have evolved fiber type-specific mechanisms to adapt Ca^{2+} sensitivity of the PTP to the cellular environment. This question, which has not been previously addressed, may be of important clinical relevance, since recent studies have shown that an increased vulnerability to opening of the PTP develops under various pathological conditions including denervation atrophy (15), myopathies related to collagen VI deficiencies (28), and Duchenne muscular dystrophy (37), as well as bupivacaine-induced myotoxicity (27).

In the present study we hypothesized that susceptibility to PTP opening would differ according to muscle phenotype. The sensitivity to Ca^{2+}-induced PTP opening was therefore measured in permeabilized muscle fibers from slow- and fast-twitch muscles with the use of a novel method that allows monitoring of PTP opening in the whole mitochondrial population within small muscle samples while they remain in a relatively well-preserved cytoarchitectural environment. Because there is evidence in the literature supporting the existence of some intrinsic mitochondrial properties across fiber types, we also evaluated whether potential variations in PTP sensitivity were associated with differences in respiratory func-

Address for reprint requests and other correspondence: Y. Burelle, Université de Montréal, Dept. of Kinesiology, PO Box 6128 Centre-Ville, Montreal, Quebec, Canada, H3C 3J7 (e-mail: yan.burelle@umontreal.ca).

The costs of publication of this article were defrayed in part by the payment of page charges. The article must therefore be hereby marked "*advertisement*" in accordance with 18 U.S.C. Section 1734 solely to indicate this fact.

tion as well as in important factors that modulate Ca^{2+} sensitivity, including ROS production, baseline mitochondrial Ca^{2+} levels, and expression of putative regulatory and structural pore components.

METHODS

Animals. All experiments on animals were approved by the Université de Montréal Institutional Animal Care Committee and were conducted according to the directives of the Canadian Council on Animal Care. The animals used in this study were male Sprague-Dawley rats (Charles River, Saint-Constant, QC, Canada), weighing 250–400 g, that were housed in an environmentally controlled room (23°C, 12:12-h light-dark cycle) and provided water and food ad libitum.

Materials. All chemicals were purchased from Sigma (St. Louis, MO) with the exception of cyclosporin A (CsA; Tocris, Ellisville, MO), calcium green-5N (Ca-green), and Amplex red (Molecular Probes, Eugene, OR).

Preparation of permeabilized muscle fibers. Skinned fibers were prepared as previously described (9). Briefly, rats were anesthetized with pentobarbital sodium (5 mg/100 g body wt ip), and the soleus and medial gastrocnemius were removed and placed into precooled *buffer A* (in mM: (2.77 CaK_2EGTA, 7.23 K_2EGTA, 6.56 $MgCl_2$, 0.5 dithiothreitol (DTT), 50 K-MES, 20 imidazol, 20 taurine, 5.3 Na_2ATP, 15 phosphocreatine, pH 7.3 at 4°C). The soleus [Sol: 87% type I, 15% IIA-IIX, 0% IIB (16)] and the superficial white portion of the medial gastrocnemius [WG: 6% type I; 45% type IIA-IIX, and 47% type IIB (16)] were quickly freeze-clamped in liquid nitrogen and stored at −80°C for subsequent enzyme analysis. Thin fiber bundles from the contralateral Sol and WG were separated along fiber orientation (in *buffer A* at 4°C). Muscle fibers were then dissected from each other with needles and incubated with mild shaking for 30 min in *buffer A* supplemented with saponin (50 μg/ml). After this permeabilization procedure, fiber bundles were washed three times for 10 min in *buffer B* (in mM: 2.77 CaK_2EGTA, 7.23 K_2EGTA, 1.38 $MgCl_2$, 3.0 K_2HPO_4, 0.5 dithiothreitol, 20 imidazole, 100 K-MES, 20 taurine, pH 7.3 at 4°C) supplemented with BSA (2 mg/ml). Fiber bundles were kept on ice in the same solution until respirometry analysis.

Preparation of permeabilized "ghost" muscle fibers. Ghost fibers without myosin were prepared as previously described (43) with minor modifications. Fiber bundles were first permeabilized with saponin and washed three times in *buffer B* as described above, and then washed three times for 10 min in *buffer C* (in mM: K-MES 80, HEPES 50, taurine 20, DTT 0.5, $MgCl_2$ 10, ATP 10, pH 7.3 at 4°C). Fibers where then incubated for 30 min with intermittent manual agitation at 4°C in *buffer D* (in mM: KCL 800, HEPES 50, taurine 20, DTT 0.5, $MgCl_2$ 10, ATP 10, pH 7.3 at 4°C) to extract myosin, washed three times in low-EGTA sucrose buffer (in mM: 250 sucrose, 10 Tris base, and 0.1 EGTA, pH 7.4), and kept on ice until use for Ca^{2+}-induced PTP opening assays.

Preparation of isolated mitochondria. Isolation of mitochondria was performed as previously described (35) with minor modifications. The plantar group of muscles was dissected from the surrounding connective tissue, rapidly removed, trimmed clean of visible connective tissue, weighed, and placed in 20 ml of ice-cold mitochondrial isolation buffer (in mM: 150 sucrose, 75 KCl, 50 Tris base, 1 KH_2PO_4, 5 $MgCl_2$, 1 EGTA, and 0.2% BSA, pH 7.2). All steps were performed at 4°C. Sol and WG muscles were minced separately with scissors, incubated for 1 min with Nagarse protease (0.2 mg/ml), and homogenized using a motor-driven Teflon pestle. The homogenate volume was completed to 40 ml with cold isolation buffer and centrifuged at 800 *g* for 10 min. The supernatant was decanted and centrifuged at 10,000 *g* for 10 min. The pellet was resuspended in 40 ml of suspension buffer (in mM: 250 sucrose, 10 Tris base, and 0.1 EGTA, pH 7.4) and centrifuged at 7,000 *g* for 6 min. This washing step was repeated twice, and the final mitochondrial pellets were resuspended in 0.3 ml of suspension buffer for WG and 0.2 ml for Sol, and protein concentrations were determined using the bicinchoninic acid method (Sigma).

Respirometry. Fiber bundles (1.0–2.5 mg dry wt) were incubated at 23°C under continuous stirring in 1 ml of *buffer B* supplemented with BSA (2 mg/ml). After baseline respiration was recorded in the absence of respiratory substrates (V_{fibers}), the following additions where sequentially made: glutamate-malate (5:2.5 mM; V_{GM}), ADP (2 mM; V_{ADP}), amytal (2 μM) or rotenone (1 μM;), succinate (10 mM; V_{succ}), CCCP (1 μM), antimycin-A (8 μM), *N*,*N*,*N*,*N*-tetramethyl-*p*-phenylenediamine (TMPD)-ascorbate (0.9:9 mM; V_{TMPD}), and KCN (1.2 mM) (see Figs. 1 and 2). At the end of each test, fibers were carefully removed from the oxygraphic cell, blotted, weighted, and frozen at −80°C until the determination of citrate synthase (CS) activity. Rates of O_2 consumption were expressed in nanomoles of O_2 per minute per milligram dry weight or per unit of CS activity to normalize for differences in mitochondrial content between fiber types. This protocol allowed the determination on each bundle of *1*) basal respiration with complex I donors (V_{GM}), *2*) maximal ADP-stimulated respiration when the respiratory chain is energized with complex I (V_{ADP}) or complex II substrates (V_{succ}), and *3*) uncoupled respiration (V_{CCCP}) and maximal complex IV activity (V_{TMPD}). Three ratios were also calculated from these respiratory rates: the acceptor control ratio (ACR), or V_{ADP}/V_{GM}, which represents the degree of coupling between oxidation and phosphorylation with complex I substrates; V_{succ}/V_{ADP}, which represents the ability of complex II substrates to stimulate phosphorylation above that observed in the presence of complex I donors; and V_{TMPD}/V_{succ}, which represents the excess capacity of complex IV relative to the maximal rate of oxidative phosphorylation. Dry weight was calculated from wet fiber weight using a dry-to-wet weight ratio of 0.23 (7). This ratio has been used previously for permeabilized fibers studies (46), and we verified its appropriateness in preliminary studies (results not shown).

Ca^{2+} challenge. To determine sensitivity to PTP opening, we submitted isolated mitochondria to progressive Ca^{2+} loading of the matrix under energized conditions according to Ichas (26) as described previously (15, 36). For this purpose, mitochondria (0.15 mg/ml) were incubated at 23°C in 1.5 ml of Ca^{2+} retention capacity (CRC) buffer (in mM: 250 sucrose, 10 Tris, 10 MOPS, 0.005 EGTA, 10 P_i-Tris, pH 7.3 at 4°C) containing glutamate-malate (5:2.5 mM) or succinate-rotenone (5 mM-1 μM). After mitochondrial Ca^{2+} uptake, we monitored the change in extramitochondrial Ca^{2+} concentration using the fluorescent probe Ca-green (1 μM; excitation-emission, 505–535 nm). At the beginning of each test, residual Ca^{2+} concentration present in the buffer was adjusted to the same level using a small amount of EGTA before adding mitochondria. After the addition of mitochondria, Ca^{2+} pulses (83 nmol/mg protein) were added at 2-min intervals until mitochondrial Ca^{2+} release caused by opening of the PTP was observed. CRC was calculated as the cumulative amount of Ca^{2+} taken by mitochondria before Ca^{2+} release. It has been established previously that this value represents a reliable index of the Ca^{2+} threshold for PTP opening in the whole mitochondrial population studied (15), and we have routinely observed that Ca^{2+} release is accompanied by complete loss of membrane potential and high-amplitude swelling (36) of the matrix, which are hallmarks of permeability transition. Of note, since several factors (such as ROS, membrane and redox potentials, adenylate concentrations, $[P_i]$, pH, and substrate selection) influence PTP opening by modulating its sensitivity to Ca^{2+}, the CRC assay provides an overall measure of PTP susceptibility but does not allow us to identify the precise regulatory mechanisms contributing to it.

Sensitivity to PTP opening also was assessed by determining CRC in mitochondria within permeabilized fibers. Similar measurements have been reported previously in permeabilized hepatocytes and various cell lines (13, 17, 23). However, in contrast to these noncontractile cells, muscle fibers possess contractile filaments and a well-

developed SR. Therefore, binding of exogenous Ca^{2+} to the contractile filaments (see RESULTS and Fig. 3*A*), as well as Ca^{2+} uptake by the SR, could interfere with the measurement of mitochondrial Ca^{2+} uptake and release. To avoid these potential problems, we determined CRC in ghost fibers, which are devoid of contractile filaments. In addition, SR Ca^{2+} uptake was effectively abolished by omitting adenylates from the incubation medium and by adding oligomycin to prevent oxidative phosphorylation from residual adenylates, which may have provided energy to support SR Ca^{2+}-ATPases (see RESULTS for further details).

For these CRC measurements, ghost fibers (0.3–1.0 mg dry fiber weight) were incubated at 23°C in a quartz microcuvette with continuous magnetic stirring in 600 μl of CRC buffer (in mM: 250 sucrose, 10 MOPS, 0.005 EGTA, 10 P_i-Tris, pH 7.3) supplemented with glutamate-malate (5:2.5 mM) and 0.5 nM oligomycin. After the addition of fibers and respiratory substrates, a single pulse of 20 nmol of Ca^{2+} was added. CRC was taken as the total amount of Ca^{2+} accumulated by mitochondria before Ca^{2+} release caused by PTP opening. CRC values were expressed per milligram of dry fiber weight and by unit of CS. [Ca^{2+}] in the cuvette was calculated from a standard curve relating [Ca^{2+}] to the fluorescence of Ca-green.

Production of ROS. Mitochondrial H_2O_2 production was measured in permeabilized fiber bundles and in isolated mitochondria with the fluorescent probe Amplex red (20 μM; excitation-emission, 563–587 nm). Fiber bundles (0.3–1.0 mg dry weight) were incubated at 37°C in a quartz microcuvette with continuous magnetic stirring in 600 μl of *buffer Z* (in mM: 110 K-MES, 35 KCl, 1 EGTA, 5 K_2HPO_4, 3 $MgCl_26H_2O$, and 0.5 mg/ml BSA, pH 7.3 at 4°C) supplemented with 1.2 U/ml horseradish peroxidase as described previously (1). Isolated mitochondria were incubated at a final concentration of 0.1 mg/ml in 2 ml of CRC buffer. The rate of H_2O_2 production was monitored before and after the addition of glutamate-malate (5:2.5 mM) or succinate (5 mM) and rotenone (1 μM). Rate of H_2O_2 production was calculated from a standard curve established in the same experimental conditions, except that fibers or isolated mitochondria were absent.

Endogenous mitochondrial Ca^{2+} content. Mitochondria from the different muscles were isolated as described in *Preparation of isolated mitochondria*, except that all buffers were free of EGTA to avoid chelating Ca^{2+}. Isolated mitochondrial pellets were diluted in 0.6 N HCl (1:10 wt/vol), homogenized with a Polytron (2 × 10 s at a setting of 3), and sonicated (2 × 10 s at 40% of maximal power output). After 30 min of incubation in boiling water, samples were centrifuged for 5 min at 10,000 *g* and the supernatant was recovered. Ca^{2+} content in the supernatant was determined spectrophotometrically (VERSAmax; Molecular Devices) using an *o*-Cresolphthalein Complexone assay according to the manufacturer's instructions (TECO Diagnostics). Results are expressed in nanomoles of Ca^{2+} per milligram of protein (15).

Enzyme assay. For the measurement of CS activity, frozen fiber bundles (1.0–2.5 mg dry wt) were homogenized with a vibrating microbead homogenizer in 200 μl of homogenization buffer (in mM: 250 sucrose, 40 KCl, 2 EGTA, and 20 Tris·HCl). Homogenate was then supplemented with 0.1% Triton X-100 and incubated on ice for 60 min. After centrifugation for 8 min at 10,000 *g*, the activity of CS was determined spectrophotometrically as previously described (9, 15) and is reported in milliunits per milligram of dry fiber weight.

Western immunoblot analysis. The protein contents of cyclophilin D (CypD), adenylate nucleotide translocator-1 (ANT-1), porin [voltage-dependent anion channel (VDAC) isoforms 1-3], and subunit VIc of complex IV [cytochrome oxidase (COX)] were determined in the isolated mitochondrial fraction. Samples were prepared for SDS-PAGE by dilutions with reducing sample buffer, followed by a 5-min immersion in near-boiling water. Proteins (20 μg/lane) were loaded and resolved on 15% polyacrylamide minigels at room temperature. The gels were transferred to a polyvinylidene difluoride membrane (Millipore). Equal sample loading was confirmed by Ponceau S stain (Sigma). The membrane was fixed for 10 min with 0.05% glutaraldehyde in Tris-buffered saline with 0.1% Tween 20 (TBS-T), blocked in TBS-T supplemented with 5% nonfat milk for CypD and VDAC or with 5% BSA for ANT-1 and COX at room temperature for 90 min, and incubated overnight at 4°C with the following primary antibodies diluted in TBS-T with 5% BSA: anti-CypD (1:1,000 dilution; Calbiochem), anti-VDAC1-3 (1:2,000 dilution; Alexis Biochemicals), anti-ANT-1 (1:1,000 dilution; Calbiochem), and anti-COX (1:2,000; Invitrogen). Membranes were then incubated for 45 min at room temperature in secondary antibody solution [1:200,000 (peroxidase goat anti-mouse) or 1:75,000 dilution (peroxidase goat anti-rabbit); Jackson ImmunoResearch]. The expression of CypD, VDAC, and ANT-1 was normalized against that of COX, which was used as a loading control. Of note, the activity of COX measured in isolated mitochondria revealed no difference between Sol and WG (7.39 ± 0.431 and 7.77 ± 0.780 mU/mg protein, respectively, $n = 5$ in each muscle, $P = 0.67$), which further justified its use as an internal control. Revelation was performed by enhanced chemiluminescence (Amersham) with film exposure times ranging from 3 to 45 min. Films were scanned and bands quantified using ImagePro software.

Statistical analysis. Results are means ± SE. Statistical differences between the two muscles were analyzed by means of two-tailed Student's *t*-tests. Significance was assumed at $P \leq 0.05$.

RESULTS

Oxidative capacity and respiratory function. Figure 1 presents the results of respirometry analyses performed on permeabilized bundles from the Sol and WG. Basal respiration rate in the absence of ADP (V_{GM}), maximal ADP-stimulated respiration in the presence of substrates for complex I (V_{ADP}) and II (V_{Succ}), uncoupled respiration (V_{CCCP}), and complex IV respiratory activity (V_{TMPD}) were all significantly lower in fibers from the WG compared with the Sol when expressed per unit of weight (Fig. 1*A*). To account for differences in mitochondrial density across muscle types, we also expressed respiration per unit of CS. The validity of this normalization was confirmed by measuring CS activity in isolated mitochondria and fiber bundles. No significant difference in CS activity was observed in mitochondria isolated from the two muscles (7.4 ± 0.4 and 7.8 ± 0.8 mU/mg protein in Sol and WG, respectively, P = NS), whereas its activity per milligram of fiber was 2.1-fold lower in the WG than in the Sol (76 ± 8 vs. 162 ± 27 mU/mg dry fibers, $P = 0.002$). As shown in Fig. 1*B*, normalization of respiration for mitochondrial density abolished the differences between the two muscles under all respiratory states. The only exception was basal respiration (V_{GM}), which became greater in WG compared with Sol. There was no significant differences in the coupling between oxidation and phosphorylation in the WG compared with the Sol (V_{ADP}/V_{GM}: 4.1 ± 1.0 vs. 3.2 ± 1.2 in Sol and WG, respectively, $P = 0.16$). Similarly, no significant differences were observed between the two fiber types for the ratio V_{succ}/V_{ADP} (1.1 ± 0.3 vs. 1.0 ± 0.4, $P = 0.3$) and COX excess capacity (2.2 ± 0.7 vs. 2.8 ± 1.1, $P = 0.6$).

Sensitivity to Ca^{2+}-induced PTP opening. Respiratory function was also assessed in ghost fibers to determine whether the procedure used for the extraction of contractile filaments had adverse effects on mitochondrial function. As shown in Fig. 2, the respiratory response of ghost fibers to the sequential addition of substrates and inhibitors was similar to that observed in permeabilized bundles, suggesting that disruption of myofilaments had little effect on mitochondria.

Preliminary experiments were then performed to validate the experimental conditions used to determine CRC in permeabil-

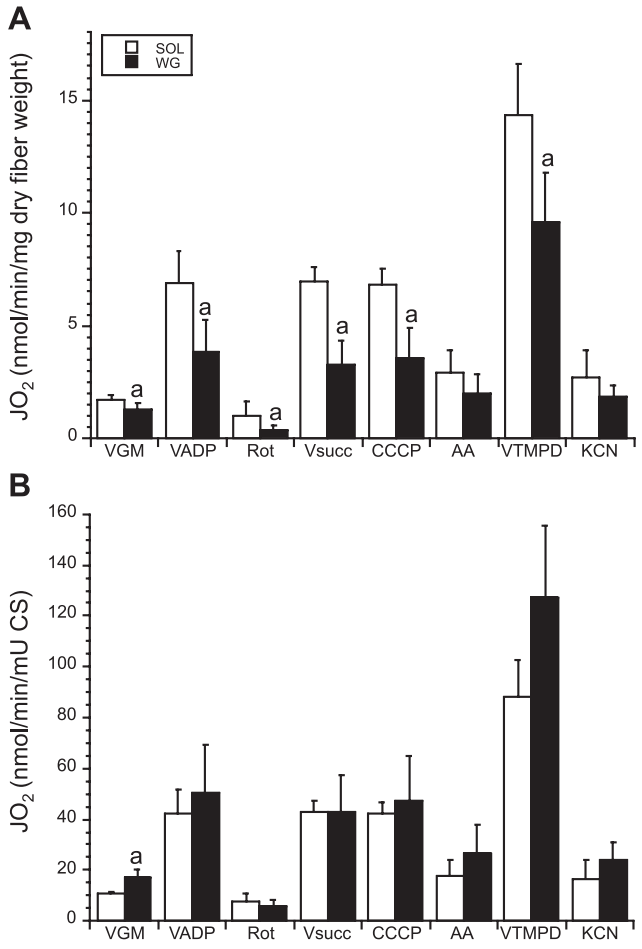

Fig. 1. Respiratory function in permeabilized fiber bundles from the soleus and white gastrocnemius. Rate of respiration (JO_2) of permeabilized fiber bundles from the soleus (Sol) and white superficial portion of the medial gastrocnemius (WG) was measured following sequential addition of glutamate-malate (V_{GM}; 5:2.5 mM), ADP (V_{ADP}; 2 mM), rotenone (Rot; 1 μM), succinate (V_{succ}; 5 mM), CCCP (1 μM), antimycin-A (AA; 8 μM), *N*,*N*,*N*,*N*-tetramethyl-*p*-phenylenediamine (TMPD)-ascorbate (V_{TMPD}; 0.9:9 mM), and potassium cyanide (KCN; 0.6 mM). Respiration is expressed per mg of dry fiber mass (*A*) or per unit of the marker enzyme citrate synthase (CS) (*B*). Values are means ± SE for $n = 5$ independent experiments per muscle. $^aP <$ 0.05, significantly different from Sol.

ized fibers. More specifically, we first determined whether the presence of contractile filaments per se could interfere with measurements of mitochondrial Ca^{2+} uptake/release by binding Ca^{2+}. This was verified by monitoring the effect of adding permeabilized (contractile filaments intact) or ghost (contractile filaments absent) fibers on the fluorescence of Ca-green under conditions in which Ca^{2+} uptake by mitochondria and SR was prevented by omitting respiratory substrates and ATP, respectively. As shown in Fig. 3*A*, addition of permeabilized fibers to the incubation medium resulted in a rapid reduction of residual Ca^{2+} present in solution, which caused an immediate drop of Ca-green fluorescence. In contrast, this reduction of fluorescence was not observed when ghost fibers were added, unless EGTA was added immediately afterward. This observation suggested that in permeabilized fibers, there was a significant amount of Ca^{2+} binding to proteins that were no longer present in ghost fibers due to the extraction of myofilaments.

Next, we determined whether changes in the fluorescence of Ca-green as a result of Ca^{2+} movements from the incubation medium to the fibers were specifically caused by Ca^{2+} uptake by mitochondria. This was verified by monitoring the effect of adding respiratory substrates and inhibitors on Ca^{2+} uptake. As shown in Fig. 3*A*, addition of 20 nmol of Ca^{2+} to either permeabilized or ghost fibers caused an increase in Ca-green fluorescence. However, in both permeabilized and ghost fibers, no uptake of Ca^{2+} was observed unless the complex I donors glutamate and malate were added to energize mitochondria. Moreover, subsequent addition of the complex I inhibitor rotenone completely abolished the uptake of Ca^{2+}, which was restored by adding succinate. The rate of Ca^{2+} uptake then reached a plateau before a release of accumulated Ca^{2+} was observed. To confirm that opening of the PTP was responsible for this Ca^{2+} release, we repeated the experiment in the presence of CsA, which desensitizes mitochondria to pore opening by binding CypD (14). As shown in Fig. 3*B*, CsA significantly increased the amount of Ca^{2+} (i.e., CRC) and time required to trigger Ca^{2+} release.

Figure 3, *C–E*, shows the time required to pore opening and the CRC measured in fibers from Sol and WG in the presence of glutamate-malate. In Sol fibers, the average time to pore opening and CRC values were 253 ± 52 s and 5.5 ± 1.1 nmol Ca^{2+}/mg dry weight, respectively. In the WG, these values were significantly higher (365 ± 51 s and 9.0 ± 2.6 Ca^{2+}/mg dry weight, respectively), despite the fact that mitochondrial volume density was about twofold lower than in the Sol. Therefore, when expressed per unit of CS, CRC values were approximately threefold higher in fibers of the WG compared with those of the Sol, indicating that mitochondria within fast-twitch glycolytic fibers were significantly less sensitive to Ca^{2+}-induced PTP opening compared with mitochondria from slow-twitch oxidative fibers.

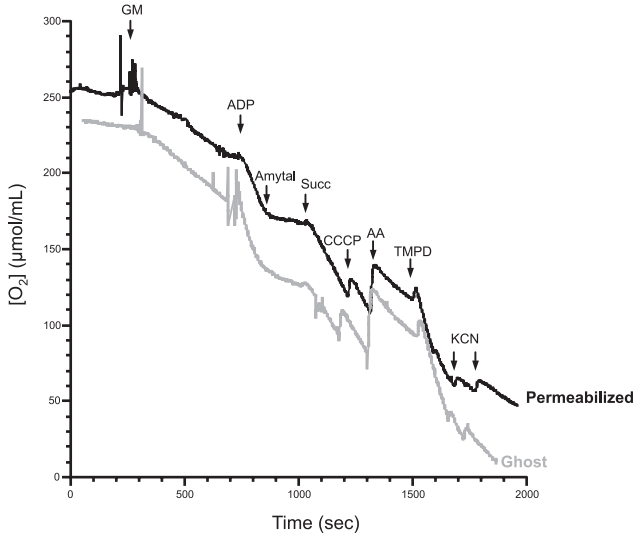

Fig. 2. Respiratory rate of permeabilized and ghost fibers. Respirometry traces were recorded from permeabilized bundles in which the contractile filaments remained intact (permeabilized) or were extracted by prior incubation in 800 KCl (ghost). The addition of substrates, inhibitors, and uncoupler is indicated above traces. The traces are representative of 5 independent preparations. The following additions are shown at the concentrations indicated in Fig. 1 legend: glutamate-malate (GM), ADP, amytal (2 μM), succinate (Succ), CCCP, AA, TMPD, and KCN.

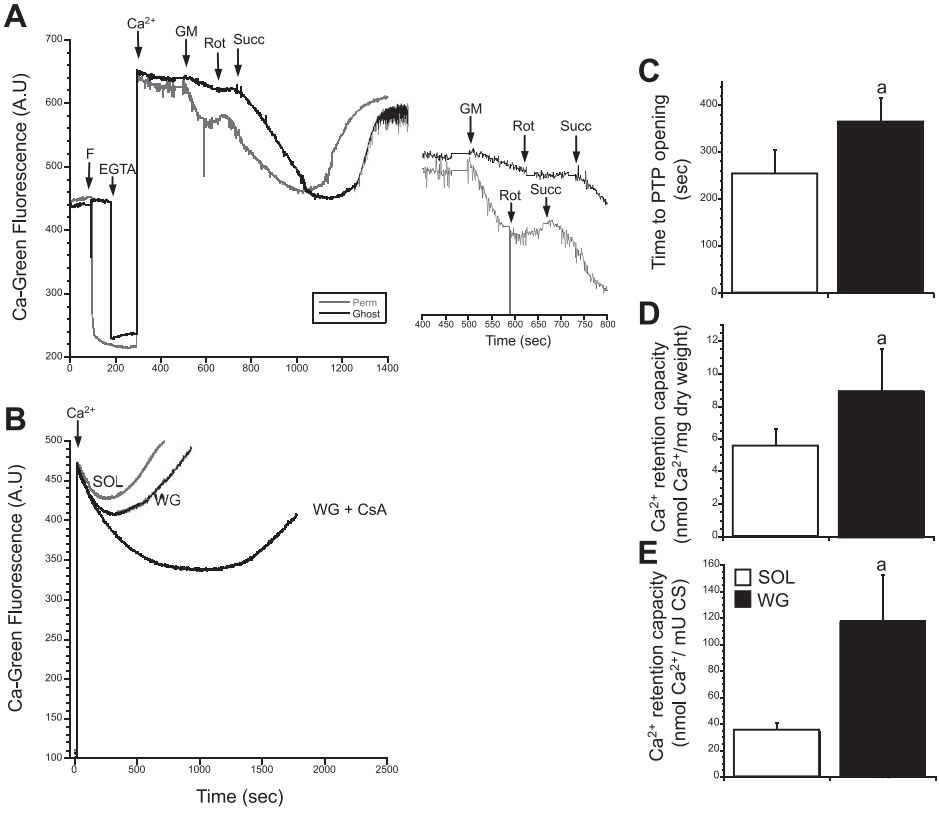

Fig. 3. Ca^{2+} uptake kinetics in permeabilized fiber bundles. *A*: changes in [Ca^{2+}] in the incubation medium in experiments performed with permeabilized bundles in which the contractile filaments were intact (Perm) or had been extracted by prior incubation in 800 KCl (ghost). The experiment was started by adding fibers (F), and the following additions were made as indicated: EGTA (4–8 μM), Ca^{2+} (20 nmol), GM (5:2.5 mM), Rot (1 μM), and Succ (5 mM). The *inset* presents an expended view of the tracing between 400 and 800 s to better show the effect of respiratory substrates and inhibitors on Ca^{2+} uptake. *B*: typical mitochondrial Ca^{2+} uptake and release following a single pulse of 20 nmol Ca^{2+} in ghost fibers from the Sol and WG. The effect of adding the PTP inhibitor cyclosporin A (CsA; 1 μM) is shown for the WG only, although a similar effect was observed with the Sol. *C*: time required to trigger pore opening, which represents the time lapse between the addition of the Ca^{2+} pulse and the time at which Ca^{2+} release was first noted. *D* and *E*: mitochondrial calcium retention capacity expressed per mg of dry fiber mass (*D*) or per unit of the mitochondrial marker CS (*E*). Values are means ± SE for $n = 5$ independent experiments per muscle. [a]$P < 0.01$, significantly different from Sol.

To confirm these observations, we also performed Ca^{2+} challenge experiments in isolated mitochondria (Fig. 4). In line with the results obtained in ghost fibers, mitochondria from WG energized with glutamate-malate were able to accumulate 121 ± 60 nmol Ca^{2+}/mg protein before PTP opening (i.e., 1.4 Ca^{2+} pulse on average; Fig. 4, *B* and *C*), whereas mitochondria isolated from Sol were unable to accumulate more than one-half of the first Ca^{2+} pulse of 83 nmol/mg protein (Fig. 4, *A* and *C*). In energized conditions, the type of substrate oxidized is known to influence Ca^{2+}-induced PTP opening, with substrates feeding complex I acting as sensitizers compared with substrates for complex II (15, 20). To determine whether this fiber type-specific PTP response was due to a difference in the sensitizing effect of complex I substrates, we also performed the experiments in the presence of the complex II donor succinate in the presence of rotenone. In line with previous results (15, 20), CRC in the presence of succinate was significantly higher than in the presence of glutamate-malate. However, the values observed in mitochondria from WG remained about twofold higher than those observed in mitochondria from Sol (456 ± 79 vs. 232 ± 16 nmol Ca^{2+}/mg protein, respectively).

Expression of PTP-related proteins. Variations in the level of expression of the PTP regulating protein CypD (3, 5, 39, 44) across tissues (liver, brain, and heart) (19) or between neurons from different regions of the brain (8) were reported to correlate with the susceptibility of mitochondria isolated from these tissues/neurons to PTP opening. Similarly, genetic modulation of ANT-1 expression was shown to alter the sensitivity to Ca^{2+}-induced PTP opening in the liver (32) and in HeLa cells (48). For these reasons, the expression of CypD, ANT-1, and VDAC isoforms 1-3 was measured in mitochondrial extracts. As shown in Fig. 5, no significant differences in the expression of CypD, ANT-1, and VDACs were observed between the two muscle types.

Production of ROS. It is well established that ROS increase the sensitivity to Ca^{2+}-induced opening of the PTP (51). Therefore, ROS production, measured as the net mitochondrial release of H_2O_2, was measured in the Sol and WG under conditions of low and high rates of H_2O_2 production, which were achieved by providing substrates for complex I and complex II donors, respectively (Fig. 6). The rate of H_2O_2 production was similar in fibers from the WG and Sol when expressed per milligram of weight (results not shown) with both the complex I donors glutamate-malate and the complex II donor succinate in the presence of rotenone. As a result, the production of H_2O_2 per unit of the mitochondrial marker enzyme CS was two- to threefold higher in fibers from WG compared with those of the Sol (Fig. 6*A*), despite the fact that the WG displayed the lowest sensitivity to PTP opening. A similar difference between the two muscles was also observed in isolated mitochondrial preparations (Fig. 6*B*).

Endogenous matrix Ca^{2+} content. Since Ca^{2+} accumulation in the matrix is a key factor triggering pore opening (51), the endogenous Ca^{2+} levels present before the Ca^{2+} challenge were determined in mitochondrial extracts. Figure 7*A* shows that endogenous Ca^{2+} levels in mitochondria from WG were 56 ± 4 nmol/mg protein, approximately twofold lower than in mitochondria from the Sol (111 ± 11 nmol/mg protein). To take this difference into account, endogenous Ca^{2+} levels were added to the CRC values measured during the in vitro Ca^{2+} challenge. As shown in Fig. 7*B*, differences in endogenous Ca^{2+} levels across muscle type significantly accounted for the greater CRC observed in mitochondria from the WG when

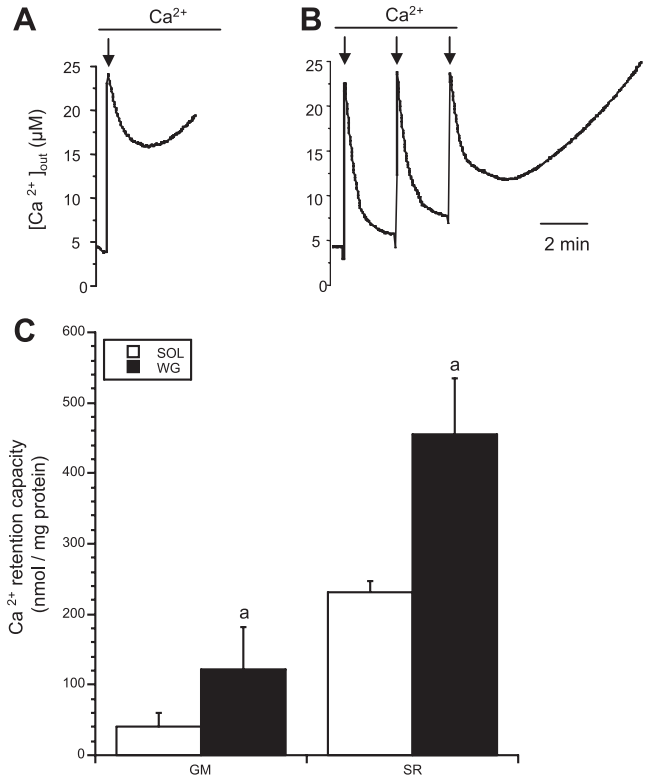

Fig. 4. Calcium retention capacity of mitochondria isolated from Sol and WG. Typical calcium green-5N tracings are shown of mitochondria (0.15 mg/ml) from the Sol (*A*) and WG (*B*) muscles energized with GM (5:2.5 mM). Tracings show progressive Ca^{2+} accumulation followed by release of accumulated Ca^{2+} secondary to PTP opening. Each spike indicates the addition of a Ca^{2+} pulse of 83 nmol/mg. Calcium retention capacity measured in several experiments in the presence of succinate-rotenone (SR) or GM is shown in *C* for each muscle. Values are means ± SE for $n = 5–6$ in each muscle. $^{a}P <$ 0.01, significantly different from the Sol.

energized with glutamate-malate. However, this was less the case when mitochondria were energized with succinate, since CRC values normalized for endogenous Ca^{2+} remained ~40% higher in the WG compared with the Sol.

DISCUSSION

In the present study, a novel method was developed to assess PTP opening under controlled conditions in the whole mitochondrial population of small muscle samples while they remain in a relatively well-preserved cytoarchitectural environment. Unlike respiratory properties, which appeared to be similar across fiber type, we found large differences in the susceptibility to Ca^{2+}-induced PTP opening, with mitochondria from fast, glycolytic WG fibers being significantly more resistant than their counterparts from slow, oxidative Sol fibers. This phenomenon was not related to differences in the expression of important putative structural and regulatory proteins of the pore and occurred despite the fact that ROS production, a factor known to favor PTP opening, was highest in the WG fibers. Our results indicate that the lower levels of endogenous matrix Ca^{2+} present in mitochondria from fast-twitch fiber play a significant role in their resistance.

Respiratory function. Quantitative and qualitative differences in mitochondrial respiratory properties across skeletal muscle fiber types have been investigated previously (4, 29, 34, 38, 45, 50). Mitochondrial volume density, determined directly or through the measurement of mitochondrial marker enzymes such as CS, is approximately twofold greater in muscles composed predominantly of type I fibers compared with muscles expressing mostly type IIb fibers (9). In contrast, the activities of CS (34, 50) and several respiratory chain complexes, including COX (34, 45) and ATP synthase (34), are relatively similar when measured in mitochondria isolated from oxidative and glycolytic muscles. In addition, mitochondria from glycolytic muscle have similar (34, 38, 41, 45, 50) or slightly lower capacities for oxidative phosphorylation (29) compared with mitochondria isolated from slow, oxidative muscles when energized with substrates feeding complex I or complex II.

In the present study, respiratory rates per unit of CS, V_{succ}/V_{ADP}, and COX excess capacity were similar in fibers from the WG and the Sol. These results are in agreement with these previous reports and indicate that variations of mitochondrial volume density, as opposed to differences in intrinsic mitochondrial properties, are the major factors accounting for the difference in oxidative capacity across fiber types. However, despite these similarities, some mitochondrial qualitative differences across fiber types have been reported previously. For example, mitochondria from oxidative muscle appear to have a greater capacity to oxidize fatty acids than their counterparts in fast fibers (29). In addition, Leary et al. (34) reported that mitochondria from fast-twitch muscle exhibited a significantly greater proton leak than their counterparts from slow, oxidative muscles. In the present study, the fact that the basal rate of respiration (V_{GM}), which is mainly driven by the proton leak, was significantly higher in the WG compared with the Sol once normalized for mitochondrial density (Fig. 1*C*) is in line with these data.

Mitochondria ROS production in slow and fast fibers. Unlike respiratory rates, the net release of H_2O_2 per milligram of fiber was comparable in the Sol and WG, under conditions of both low (glutamate-malate) and high (succinate) superoxide production (data not shown). Therefore, the production of ROS per unit of CS was significantly higher in the WG than in the Sol (Fig. 6*A*), which is consistent with the greater rate of H_2O_2 per unit of O_2 consumed recently reported by Anderson and Neufer (1) in permeabilized fibers from the WG compared with the Sol. Although the mechanisms responsible for this difference were not investigated in the present study, Anderson and Neufer (1) reported using permeabilized fibers from the same muscles, so this could in part be attributable to the fact that fibers from the WG have a lower total H_2O_2 scavenging capacity than those of the Sol. In the present study, the fact that we observed the same fiber-type differences in permeabilized fibers and isolated mitochondria clearly indicates that intrinsic mitochondrial differences (i.e., increased H_2O_2 production and/or reduced removal), rather than extramitochondrial factors present in permeabilized fibers, were responsible for the potentiation of H_2O_2 efflux in fast-twitch fibers.

Measurement of PTP opening in ghost fibers. Extraction of myosin by incubation in presence of high concentrations of KCl has been used previously to study mitochondrial function. Electron microscopy and confocal imaging experiments have shown that this procedure effectively removes myosin and entirely disrupts contractile proteins, while mitochondria remain attached to the cytoskeleton, retain their original local-

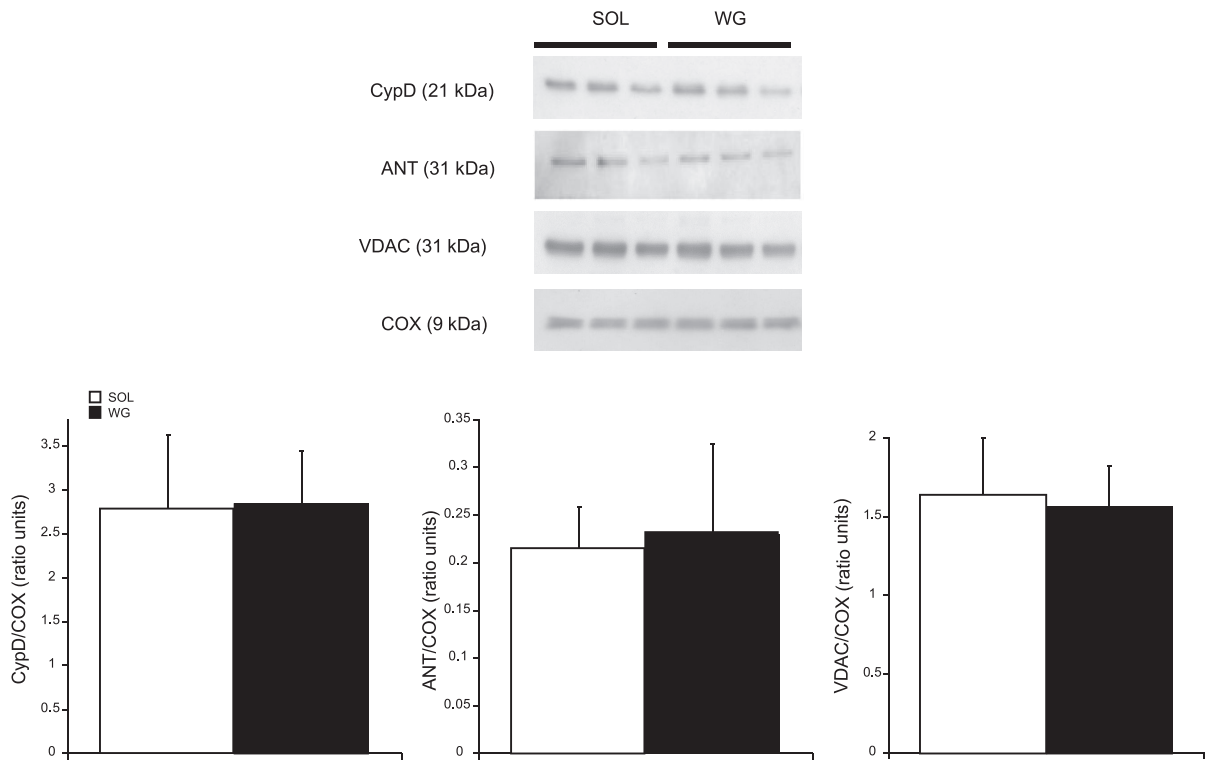

Fig. 5. Cyclophilin D (CypD), voltage-dependent cation channel (VDAC) and adenine nucleotide translocase (ANT) content of mitochondrial fraction from the Sol and WG. Representative immunoblots of CypD (21 kDa), VDAC (31 kDa), ANT (31 kDa), and subunit VIc of cytochrome oxidase (COX; 9 kDa) are shown in mitochondrial fractions isolated from the Sol and WG muscles. The expression level of CypD, VDAC, and ANT is normalized against that of COX, which was used as a loading control. Values represent optical density and are means ± SE for $n = 6$ in each muscle.

ization within the myocytes, and maintain normal respiratory parameters (2, 42, 43). However, the present study is the first to use ghost fibers to determine mitochondrial sensitivity to Ca^{2+}-induced PTP opening. One advantage of this method over isolated mitochondria is the small amount of tissue required (0.2–0.5 mg dry mass), which makes it interesting for studies in human muscle biopsies or mice skeletal muscle. In addition, because the whole population of mitochondria is studied in a relatively preserved environment, possible selection bias caused by the isolation methods is avoided.

In the present study we found evidence that supports the validity of this approach. First, we confirmed that disruption of contractile proteins was not associated with any deleterious effects on mitochondria, as judged by the absence of deterioration of respiratory function (Fig. 2). Importantly, the uptake of Ca^{2+} measured was entirely dependent on the presence of respiratory substrates and was inhibited by rotenone (Fig. 3), indicating that mitochondria were the major contributor to the removal of Ca^{2+} in ghost fibers. Another organelle that could have taken up Ca^{2+} is the SR. However, by omitting adenylates from the incubation medium and by adding oligomycin to prevent oxidative phosphorylation, any contribution of SERCA pumps to Ca^{2+} uptake could be ruled out. Finally, CRC was considerably increased by CsA, which confirmed that the release of Ca^{2+} was caused by opening of the PTP. Of note, in preliminary studies, we also observed an uptake of Ca^{2+} by mitochondria in permeabilized non-ghost fibers (Fig. 3*A*). However, there was also a significant chelation of Ca^{2+} that occurred in the absence of respiratory substrates. Because this phenomenon did not occur in ghost fibers, we believe that it was caused by the binding of Ca^{2+} to proteins associated with the contractile apparatus. Given that Ca^{2+} binding to these proteins varies according to fiber type (6), we suggest that the use of ghost fibers is preferable.

Sensitivity to PTP opening in fast and slow fibers. Using this approach, we observed that the time required to trigger PTP opening following the addition of Ca^{2+} was ~30% longer and that the CRC per unit of CS was more than three times higher in the WG compared with the Sol. This resistance of WG fibers to PTP opening was also observed in isolated mitochondria, which indicates that it is linked to differences in mitochondrial factors between the two muscles. To our knowledge, this is the first study to report fiber-type differences in the intrinsic susceptibility to Ca^{2+}-induced PTP opening. However, interestingly, muscle fibers with a fast glycolytic phenotype (e.g., extensor digitorum longus and esophageal muscles) were reported to be less sensitive to the myotoxic effects of bupivacaine, a local anesthetic agent with potent pore-inducing effects (27). The authors hypothesized that this could be due to the fact that fast-twitch fibers contain less mitochondria and rely more on glycolysis to support their energy requirements than slow-twitch fibers. Although this explanation is plausible, the present results indicate that this also could be due to the fact that mitochondria from fast-twitch muscles are intrinsically less prone to undergo permeability transition in the presence of Ca^{2+} than their counterparts in slow, oxidative muscles, at least in this particular condition.

Mitochondrial permeability transition is influenced by several parameters (51) that may confer tissue- and cell type-specific regulation. Variations in the expression of the PTP-

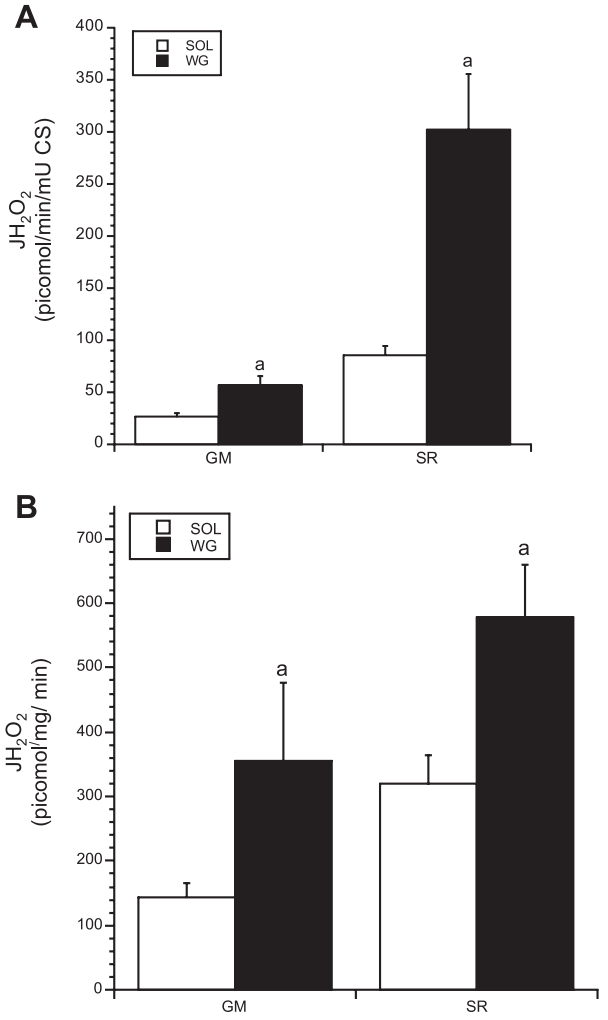

Fig. 6. Mitochondrial H_2O_2 production. H_2O_2 production was measured in permeabilized fibers (*A*) and isolated mitochondria (*B*) from the WG and SOL when energized with substrates for complex II (SR, 5 mM:1 μM) or complex I (GM, 5:2.5 mM). For permeabilized fibers, rates of H_2O_2 production (JH_2O_2) are expressed per unit of the mitochondrial marker enzyme CS, whereas for isolated mitochondria, rates are expressed per mg of protein. Data are means ± SE; $n = 5$ and 9 for each muscle for permeabilized fibers and isolated mitochondria, respectively. $^aP < 0.05$, significantly different from Sol.

regulating protein CypD (3, 5, 39, 44) across tissues (liver, brain, and heart) (19) or between neurons from different regions of the brain (8) were recently reported to correlate with the susceptibility of mitochondria isolated from these tissues/neurons to PTP opening. Similarly, genetic modulation of ANT expression was shown to alter the sensitivity to Ca^{2+}-induced PTP opening in the liver (32) and in HeLa cells (48). However, to our knowledge, the question of whether the expression of these proteins varies across fiber types has not been investigated previously. The similar expression levels of CypD, ANT-1, and VDACs observed in mitochondria from the Sol and WG in the present study clearly suggest that in skeletal muscle, variations in the expression of these proteins between cell types cannot account for their different susceptibilities to permeability transition, as has been reported in neurons for CypD (8). Of note, although ANT-1 is the main isoform present in skeletal muscle, ANT-3 is expressed in small amounts in virtually all tissues (48). Therefore, our data cannot exclude the possibility that the difference in susceptibility to pore opening is related to different expression levels of this isoform across fiber type.

Production of ROS is another factor that could have played a role, since oxidative stress is well known to promote opening of the PTP in the presence of Ca^{2+} by their strong oxidizing action on critical SH residues of pore-forming proteins (51). However, we observed that mitochondria from the WG were actually more resistant to Ca^{2+}-induced opening of the PTP, despite the fact that they produced more H_2O_2 than their counterparts from the Sol. These results thus rule out the contribution of ROS as a mechanism to explain fiber-type differences in PTP susceptibility and suggest that other, more influential factors are involved.

Calcium is a critical factor favoring permeability transition (51). In fast glycolytic fibers, $[Ca^{2+}]$ in the cytosol under

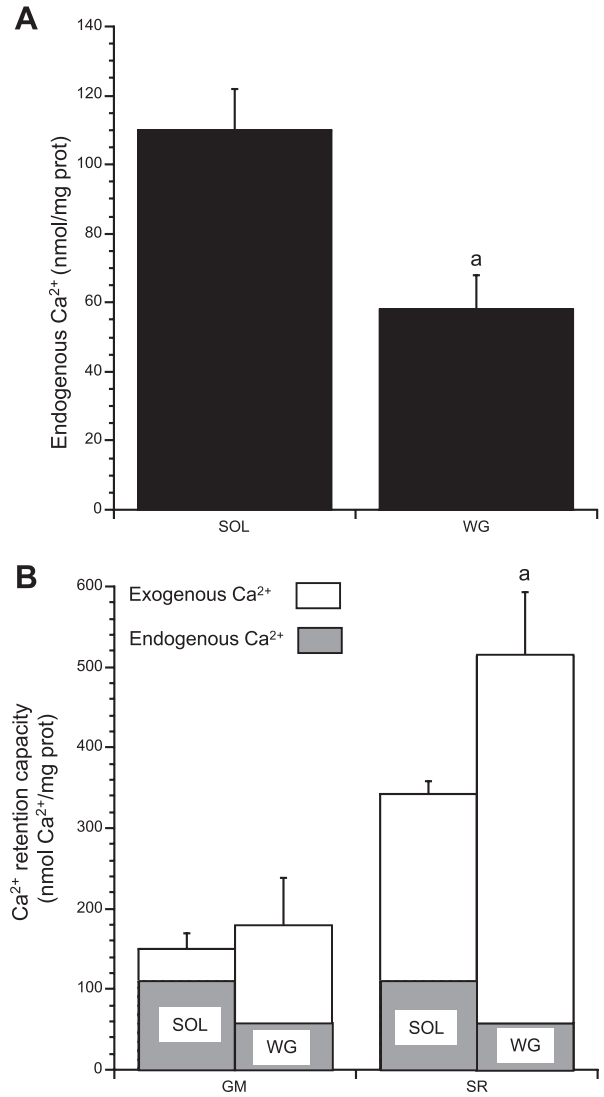

Fig. 7. Endogenous mitochondrial Ca^{2+} content and its contribution to calcium retention capacity. *A*: endogenous Ca^{2+} content measured in the mitochondrial fraction of Sol and WG muscles. *B*: total calcium retention capacity expressed as the sum of the contribution of endogenous mitochondrial Ca^{2+} and the exogenous Ca^{2+} added during the in vitro challenge in isolated mitochondria. Data are means ± SE; $n = 5$–6 for each muscle. $^aP < 0.05$, significantly different from Sol.

noncontracting conditions was reported to be lower than in slow-twitch fibers because of the higher capacity of the SR for Ca^{2+} uptake and the presence of the cytosolic Ca^{2+}-binding protein parvalbumin (10, 11, 21). For this reason, the steady-state Ca^{2+} level in mitochondria at rest may be lower in fast-twitch fibers, as suggested in the present study by the twofold lower endogenous Ca^{2+} levels in mitochondrial extracts from the WG compared with those of the Sol (Fig. 7). Importantly, the difference (Δ) in endogenous Ca^{2+} content between mitochondria from the WG and Sol (Δ = 57 nmol Ca^{2+}/mg protein) was close to the difference in CRC observed between the two muscles when isolated mitochondria were energized with glutamate-malate (Δ = 40 nmol Ca^{2+}/mg protein, range 20–73 nmol Ca^{2+}/mg protein), which indicates that lower endogenous Ca^{2+} levels likely represent an important factor responsible for the resistance of mitochondria from the WG to PTP opening.

However, in the presence of glutamate-malate, CRC is relatively low due to the sensitizing effect of complex I substrates on pore opening (20). Therefore, this experimental condition tends to increase the relative importance of endogenous Ca^{2+} in determining the sensitivity to PTP opening. In contrast, when succinate is used to bypass complex I, CRC values are significantly higher (Fig. 4 and Refs. 15, 20), and endogenous Ca^{2+} levels therefore play a comparatively smaller role in determining PTP sensitivity (Fig. 6). In this situation, we observed that the difference in endogenous Ca^{2+} content could not fully account for the difference in CRC observed between the WG and the Sol (Δendogenous Ca^{2+}: 57 nmol Ca^{2+}/mg protein vs. ΔCRC = 224 nmol Ca^{2+}/mg protein, range 166–581 nmol Ca^{2+}/mg protein). Therefore, our results indicate that the difference in endogenous matrix Ca^{2+} levels does not appear to be the only contributor to this phenomenon and that other factors, which remain to be identified, are likely involved.

Perspective and Significance

In summary, our results support the idea that in skeletal muscle, the sensitivity of the PTP to Ca^{2+}-induced opening varies according to fiber type. Since transient opening of the PTP is believed to play a physiological role in the regulation of mitochondrial (e.g., $\Delta\Psi$, ROS production, ion homeostasis) function and cell Ca^{2+} signaling (33), a higher Ca^{2+} threshold for PTP opening in fast fibers may represent a mechanism to adapt PTP responses to the higher Ca^{2+} surges that occur during high-frequency contractions in this fiber type under physiological conditions of repeated recruitment. Further studies in intact muscle fibers are required to confirm this hypothesis.

On the other hand, the implication of this phenomenon in muscle pathology remains unclear. Indeed, under certain conditions such as exposure to bupivacaine, the greater resistance to PTP opening we observed in fast fibers could clearly contribute to explain why mitochondrial dysfunction and myotoxicity appear to be less important in these fibers than in those with a slow-twitch phenotype (27). On the other hand, this resistance of fast fibers is in apparent contradiction with the observation that in other pathological states such as ischemia-reperfusion (12, 49) and Duchenne muscular dystrophy (47), in which PTP opening plays a role in injury (18, 37), type II fibers appear to be more affected than type I fibers. A likely explanation for this phenomenon is that alterations in cellular factors that promote PTP opening are greater in fast fibers than in slow fibers as a result of these pathological states and overwhelm the capacity of mitochondria to resist to permeability transition. Clearly, the involvement of mitochondria in cell death depends on the convergence of several factors, and further studies are required to better establish their role in various muscle pathologies. The novel method we have described that allows assessment of PTP sensitivity in small muscle samples will facilitate these investigations in mouse models of disease and in human biopsy samples.

ACKNOWLEDGMENTS

We thank Dr. Tanja Taivassalo for her contribution to this study.

GRANTS

This work was supported by Natural Sciences and Engineering Council of Canada Grant 261864-03. Y. Burelle is a Junior 2 Investigator of the Fonds de Recherche en Santé du Québec.

REFERENCES

1. **Anderson EJ, Neufer PD.** Type II skeletal myofibers possess unique properties that potentiate mitochondrial H_2O_2 generation. *Am J Physiol Cell Physiol* 290: C844–C851, 2006.
2. **Andrienko T, Kuznetsov AV, Kaambre T, Usson Y, Orosco A, Appaix F, Tiivel T, Sikk P, Vendelin M, Margreiter R, Saks VA.** Metabolic consequences of functional complexes of mitochondria, myofibrils and sarcoplasmic reticulum in muscle cells. *J Exp Biol* 206: 2059–2072, 2003.
3. **Baines CP, Kaiser RA, Purcell NH, Blair NS, Osinska H, Hambleton MA, Brunskill EW, Sayen MR, Gottlieb RA, Dorn GW, Robbins J, Molkentin JD.** Loss of cyclophilin D reveals a critical role for mitochondrial permeability transition in cell death. *Nature* 434: 658–662, 2005.
4. **Baldwin KM, Klinkerfuss GH, Terjung RL, Mole PA, Holloszy JO.** Respiratory capacity of white, red, and intermediate muscle: adaptative response to exercise. *Am J Physiol* 222: 373–378, 1972.
5. **Basso E, Fante L, Fowlkes J, Petronilli V, Forte MA, Bernardi P.** Properties of the permeability transition pore in mitochondria devoid of cyclophilin D. *J Biol Chem* 280: 18558–18561, 2005.
6. **Baylor SM, Hollingworth S.** Sarcoplasmic reticulum calcium release compared in slow-twitch and fast-twitch fibres of mouse muscle. *J Physiol* 551: 125–138, 2003.
7. **Bergström J.** Muscle electrolytes in man. *Scand J Clin Lab Invest* 68, *Suppl*: 1–101, 1962.
8. **Brustovetsky N, Brustovetsky T, Purl KJ, Capano M, Crompton M, Dubinsky JM.** Increased susceptibility of striatal mitochondria to calcium-induced permeability transition. *J Neurosci* 23: 4858–4867, 2003.
9. **Burelle Y, Hochachka PW.** Endurance training induces muscle-specific changes in mitochondrial function in skinned muscle fibers. *J Appl Physiol* 92: 2429–2438, 2002.
10. **Carroll S, Nicotera P, Pette D.** Calcium transients in single fibers of low-frequency stimulated fast-twitch muscle of rat. *Am J Physiol Cell Physiol* 277: C1122–C1129, 1999.
11. **Carroll SL, Klein MG, Schneider MF.** Decay of calcium transients after electrical stimulation in rat fast- and slow-twitch skeletal muscle fibres. *J Physiol* 501: 573–588, 1997.
12. **Chan RK, Austen WG Jr, Ibrahim S, Ding GY, Verna N, Hechtman HB, Moore FD, Jr.** Reperfusion injury to skeletal muscle affects primarily type II muscle fibers. *J Surg Res* 122: 54–60, 2004.
13. **Chauvin C, De Oliveira F, Ronot X, Mousseau M, Leverve X, Fontaine E.** Rotenone inhibits the mitochondrial permeability transition-induced cell death in U937 and KB cells. *J Biol Chem* 276: 41394–41398, 2001.
14. **Crompton M.** The mitochondrial permeability transition pore and its role in cell death. *Biochem J* 341: 233–249, 1999.
15. **Csukly K, Ascah A, Matas J, Gardiner PF, Fontaine E, Burelle Y.** Muscle denervation promotes opening of the permeability transition pore and increases the expression of cyclophilin D. *J Physiol* 574: 319–327, 2006.

16. **Delp MD, Duan C.** Composition and size of type I, IIA, IID/X, and IIB fibers and citrate synthase activity of rat muscle. *J Appl Physiol* 80: 261–270, 1996.
17. **Detaille D, Guigas B, Chauvin C, Batandier C, Fontaine E, Wiernsperger N, Leverve X.** Metformin prevents high-glucose-induced endothelial cell death through a mitochondrial permeability transition-dependent process. *Diabetes* 54: 2179–2187, 2005.
18. **Di Lisa F, Bernardi P.** Mitochondrial function as a determinant of recovery or death in cell response to injury. *Mol Cell Biochem* 184: 379–391, 1998.
19. **Eliseev RA, Filippov G, Velos J, VanWinkle B, Goldman A, Rosier RN, Gunter TE.** Role of cyclophilin D in the resistance of brain mitochondria to the permeability transition. *Neurobiol Aging* 28: 1532–1542, 2007.
20. **Fontaine E, Eriksson O, Ichas F, Bernardi P.** Regulation of the permeability transition pore in skeletal muscle mitochondria. Modulation by electron flow through the respiratory chain complex I. *J Biol Chem* 273: 12662–12668, 1998.
21. **Fryer MW, Stephenson DG.** Total and sarcoplasmic reticulum calcium contents of skinned fibres from rat skeletal muscle. *J Physiol* 493: 357–370, 1996.
22. **Green DR, Kroemer G.** The pathophysiology of mitochondrial cell death. *Science* 305: 626–629, 2004.
23. **Guigas B, Detaille D, Chauvin C, Batandier C, De Oliveira F, Fontaine E, Leverve X.** Metformin inhibits mitochondrial permeability transition and cell death: a pharmacological in vitro study. *Biochem J* 382: 877–884, 2004.
24. **Haworth RA, Hunter DR.** The Ca^{2+}-induced membrane transition in mitochondria. II. Nature of the Ca^{2+} trigger site. *Arch Biochem Biophys* 195: 460–467, 1979.
25. **Hengartner MO.** The biochemistry of apoptosis. *Nature* 407: 770–776, 2000.
26. **Ichas F, Jouaville LS, Mazat JP.** Mitochondria are excitable organelles capable of generating and conveying electrical and calcium signals. *Cell* 89: 1145–1153, 1997.
27. **Irwin W, Fontaine E, Agnolucci L, Penzo D, Betto R, Bortolotto S, Reggiani C, Salviati G, Bernardi P.** Bupivacaine myotoxicity is mediated by mitochondria. *J Biol Chem* 277: 12221–12227, 2002.
28. **Irwin WA, Bergamin N, Sabatelli P, Reggiani C, Megighian A, Merlini L, Braghetta P, Columbaro M, Volpin D, Bressan GM, Bernardi P, Bonaldo P.** Mitochondrial dysfunction and apoptosis in myopathic mice with collagen VI deficiency. *Nat Genet* 35: 367–371, 2003.
29. **Jackman MR, Willis WT.** Characteristics of mitochondria isolated from type I and type IIb skeletal muscle. *Am J Physiol Cell Physiol* 270: C673–C678, 1996.
30. **Jouaville LS, Ichas F, Mazat JP.** Modulation of cell calcium signals by mitochondria. *Mol Cell Biochem* 184: 371–376, 1998.
31. **Kim JS, He L, Lemasters JJ.** Mitochondrial permeability transition: a common pathway to necrosis and apoptosis. *Biochem Biophys Res Commun* 304: 463–470, 2003.
32. **Kokoszka JE, Waymire KG, Levy SE, Sligh JE, Cai J, Jones DP, MacGregor GR, Wallace DC.** The ADP/ATP translocator is not essential for the mitochondrial permeability transition pore. *Nature* 427: 461–465, 2004.
33. **Korshunov SS, Skulachev VP, Starkov AA.** High protonic potential actuates a mechanism of production of reactive oxygen species in mitochondria. *FEBS Lett* 416: 15–18, 1997.
34. **Leary SC, Lyons CN, Rosenberger AG, Ballantyne JS, Stillman J, Moyes CD.** Fiber-type differences in muscle mitochondrial profiles. *Am J Physiol Regul Integr Comp Physiol* 285: R817–R826, 2003.
35. **Madsen K, Ertbjerg P, Pedersen PK.** Calcium content and respiratory control index of isolated skeletal muscle mitochondria: effects of different isolation media. *Anal Biochem* 237: 37–41, 1996.
36. **Marcil M, Bourduas K, Ascah A, Burelle Y.** Exercise training induces respiratory substrate-specific decrease in Ca^{2+}-induced permeability transition pore opening in heart mitochondria. *Am J Physiol Heart Circ Physiol* 290: H1549–H1557, 2006.
37. **Millay DP, Sargent MA, Osinska H, Baines CP, Barton ER, Vuagniaux G, Sweeney HL, Robbins J, Molkentin JD.** Genetic and pharmacologic inhibition of mitochondrial-dependent necrosis attenuates muscular dystrophy. *Nat Med* 14: 442–447, 2008.
38. **Mogensen M, Sahlin K.** Mitochondrial efficiency in rat skeletal muscle: influence of respiration rate, substrate and muscle type. *Acta Physiol Scand* 185: 229–236, 2005.
39. **Nakagawa T, Shimizu S, Watanabe T, Yamaguchi O, Otsu K, Yamagata H, Inohara H, Kubo T, Tsujimoto Y.** Cyclophilin D-dependent mitochondrial permeability transition regulates some necrotic but not apoptotic cell death. *Nature* 434: 652–658, 2005.
40. **Ogata T, Yamasaki Y.** Ultra-high-resolution scanning electron microscopy of mitochondria and sarcoplasmic reticulum arrangement in human red, white, and intermediate muscle fibers. *Anat Rec* 248: 214–223, 1997.
41. **Pande SV, Blanchaer MC.** Carbohydrate and fat in energy metabolism of red and white muscle. *Am J Physiol* 220: 549–553, 1971.
42. **Saks VA, Khuchua ZA, Vasilyeva EV, Belikova O, Kuznetsov AV.** Metabolic compartmentation and substrate channelling in muscle cells. Role of coupled creatine kinases in in vivo regulation of cellular respiration—a synthesis. *Mol Cell Biochem* 133–134: 155–192, 1994.
43. **Saks VA, Veksler VI, Kuznetsov AV, Kay L, Sikk P, Tiivel T, Tranqui L, Olivares J, Winkler K, Wiedemann F, Kunz WS.** Permeabilized cell and skinned fiber techniques in studies of mitochondrial function in vivo. *Mol Cell Biochem* 184: 81–100, 1998.
44. **Schinzel AC, Takeuchi O, Huang Z, Fisher JK, Zhou Z, Rubens J, Hetz C, Danial NN, Moskowitz MA, Korsmeyer SJ.** Cyclophilin D is a component of mitochondrial permeability transition and mediates neuronal cell death after focal cerebral ischemia. *Proc Natl Acad Sci USA* 102: 12005–12010, 2005.
45. **Schwerzmann K, Hoppeler H, Kayar SR, Weibel ER.** Oxidative capacity of muscle and mitochondria: correlation of physiological, biochemical, and morphometric characteristics. *Proc Natl Acad Sci USA* 86: 1583–1587, 1989.
46. **Walsh B, Tonkonogi M, Malm C, Ekblom B, Sahlin K.** Effect of eccentric exercise on muscle oxidative metabolism in humans. *Med Sci Sports Exerc* 33: 436–441, 2001.
47. **Webster C, Silberstein L, Hays AP, Blau HM.** Fast muscle fibers are preferentially affected in Duchenne muscular dystrophy. *Cell* 52: 503–513, 1988.
48. **Wieckowski MR, Szabadkai G, Wasilewski M, Pinton P, Duszynski J, Rizzuto R.** Overexpression of adenine nucleotide translocase reduces Ca^{2+} signal transmission between the ER and mitochondria. *Biochem Biophys Res Commun* 348: 393–399, 2006.
49. **Woitaske MD, McCarter RJ.** Effects of fiber type on ischemia-reperfusion injury in mouse skeletal muscle. *Plast Reconstr Surg* 102: 2052–2063, 1998.
50. **Yajid F, Mercier JG, Mercier BM, Dubouchaud H, Prefaut C.** Effects of 4 wk of hindlimb suspension on skeletal muscle mitochondrial respiration in rats. *J Appl Physiol* 84: 479–485, 1998.
51. **Zoratti M, Szabo I.** The mitochondrial permeability transition. *Biochim Biophys Acta* 1241: 139–176, 1995.
52. **Zoratti M, Szabo I, De Marchi U.** Mitochondrial permeability transitions: how many doors to the house? *Biochim Biophys Acta* 1706: 40–52, 2005.